UNIVERSITY OF WOLVERHAMPTON

Compressive characteristics of perforated re-entrant auxetic steel honeycomb–mortar composite

Item Type	Conference contribution
Authors	Momoh, Emmanuel Owoichoechi;Hajsadeghi, Mohammad;Jayasinghe, Amila;Vinai, Raffaele;Kripakaran, Prakash;Orr, John;Evans, Ken
Citation	Momoh, E.O. et al. (2025). Compressive Characteristics of Perforated Re-entrant Auxetic Steel Honeycomb–Mortar Composite. In: Kioumarsi, M., Shafei, B. (eds) The 1st International Conference on Net-Zero Built Environment. NTZR 2024. Lecture Notes in Civil Engineering, vol 237. Springer, Cham. https://doi.org/10.1007/978-3-031-69626-8_21
DOI	10.1007/978-3-031-69626-8_21
Publisher	Springer Nature
Download date	2026-01-13 07:14:15
License	https://creativecommons.org/licenses/by/4.0/
Link to Item	http://hdl.handle.net/2436/625833

Compressive Characteristics of Perforated Re-entrant Auxetic Steel Honeycomb–Mortar Composite

Emmanuel Owoichoechi Momoh, Mohammad Hajsadeghi, Amila Jayasinghe, Raffaele Vinai, Prakash Kripakaran, John Orr, and Ken E. Evans

Contents

1 Introduction

Cementitious materials are the most used construction materials due to their relatively low cost and ease of production, which essentially requires fluid concrete to be poured into moulds and be allowed to set [1, 2]. Although excellent in compressive strength, the inherent brittleness and poor tensile strength of these materials result in low energy absorption and sudden fracture when the material tensile strength is exceeded. Consequently, cementitious materials are unsuitable for high-energy absorption applications such as vibration and impact resistance. Several approaches have been employed to improve the ductility for such brittle materials, such as through embedding of ductile reinforcement materials, e.g. steel rods, steel strands

E. O. Momoh (✉) · M. Hajsadeghi · R. Vinai · P. Kripakaran · K. E. Evans
Department of Engineering, Faculty of Environment Science, and Economy, University of Exeter, Exeter, UK
e-mail: e.o.momoh@exeter.ac.uk

A. Jayasinghe · J. Orr
Department of Engineering, University of Cambridge, Cambridge, UK

© The Author(s) 2025

M. Kioumarsi, B. Shafei (eds.), *The 1st International Conference on Net-Zero Built Environment*, Lecture Notes in Civil Engineering 237,
https://doi.org/10.1007/978-3-031-69626-8_21

and fibres [3], polymers [4, 5], natural fibres [6, 7] and only recently auxetic materials derived from altering the geometries of conventional materials [2, 8]. While conventional materials expand laterally when compressed axially and contract laterally under axial tension, auxetic materials contract laterally when compressed axially and expand laterally under axial tension. This counter intuitive behaviour of auxetic materials that results in Negative Poisson's Ratio (NPR) can be exploited for enhancing indentation resistance [9, 10], shear resistance [9, 11], strain-hardening, energy absorption, crashworthiness, damping [9, 12, 13]; as well as physical characteristics such as acoustic behaviour [11] and inherent synclasticity under bending moments [13].

Auxetic behaviour has been cheaply achieved in several studies by altering the geometry of conventional materials. The most studied auxetic geometry with potential application in structural engineering is the re-entrant honeycomb structure [14]. Several studies have investigated re-entrant honeycomb structures with concrete infill. The study of Zhong et al. [15] investigated the compressive strength behaviour of fabricated re-entrant honeycomb aluminium structures with 0.4 mm of sheet thickness. The height and width of the re-entrant honeycomb structure were 110 mm and filled with 16 MPa concrete. The elastic modulus and tensile strength of the aluminium sheets were 69 GPa and 274 MPa, respectively. The study reported the enhancement of the composite against compression, buckling, flexure and shear failures. The study investigated the confinement effect of the auxetic honeycomb lattice to the transverse deformation of the concrete matrix. The influence of dimensional parameters such as cell wall thickness, cell angle and cell size on the auxetic response of the composite was also investigated. The method of manufacture of the aluminium re-entrant honeycomb was firstly by folding plain sheets of aluminium, then stacking and gluing the folded sheets. The same type of honeycomb was used in the study of Zhou et al. [16], although with foam concrete as the cementitious matrix. Zhou et al. [16] investigated the in-plane uniaxial quasi-static and dynamic compressive strength of the auxetic mesh-reinforced foam concrete. The sample failure evolved from predominantly compression to shear especially as the density of the foam concrete increased. The study recommended the use of auxetic meshes to enhance load-bearing of porous cementitious structures.

Apart from sheet folding and crimping into re-entrant shapes, another popular method of introducing auxetic behaviour in metal sheets is through perforations. Perforations in the form of orthogonal ellipses have been shown to create nodes of rotation within the perforation grids and hence cause NPR [14, 17]. For example, in the study of Luo et al. [17], 8 mm, 10 mm and 12 mm thick stainless steel sheets were perforated in orthogonal alternating elliptic patterns (using laser cutting technology) and folded into tubes. The tubes were then filled with concrete and tested in compression after 28 days. The elliptical-perforated tubes were compared with circular-perforated tubes with the same area of perforations. The elliptical-perforated tubes provided active restraint to the lateral strain of the concrete, thereby enhancing the axial compressive strength of the composite.

Investigations of auxetic behaviour through perforation of materials are scarce and focused on tubular structures used as external confinement to the cementitious phase. Also in such studies, the auxetic behaviour is limited to the material plane of the confinement. This means that, apart from the confining edge provided by the sheet metal, the greater volume of the cementitious phase is unaffected by the auxetic behaviour of the sheet metal. Furthermore, for structures such as re-entrant honeycombs, there is lack of continuity in the cementitious matrix as each cell is separated by a continuous sheet of metal. In this study, the possibility of introducing auxeticity throughout the composite in re-entrant honeycomb structures through perforations is explored. The perforations are also expected to enhance the bond strength between the metal sheet and the cementitious matrix, as well as additional confinement, thereby improving the mechanical properties of the overall composite.

The effect of the perforations on the compressive capacities of the samples is investigated by comparing the force–displacement curves of the circular-perforated, elliptic-perforated and peanut-perforated samples with the non-perforated samples. Subsequent paragraphs, however, are indented.

2 Materials and Methods

2.1 Re-entrant Honeycomb Structure

Cold-reduced (CR4) steel sheets of 0.9 mm thickness were supplied by The Metal Store, UK, and cut into strips of 1200 × 70 mm and used for the non-perforated samples. For the perforated samples, a plasma cutter was used to carry out the perforations before the sheet was cut into the 1200 × 70 mm strips. All the perforated samples have the same volume of materials which is exactly half the volume of the non-perforated samples. Details of the dimensions of the sheets and perforations are shown in Fig. 1.

For both perforated and non-perforated sheets, the samples were folded into re-entrant shapes at 75° angle of inclination as shown in Fig. 2i. The folded metal sheets were stacked upon one another and welded using TIG welding. Non-perforated solid plates of the same thickness were welded on to the top and

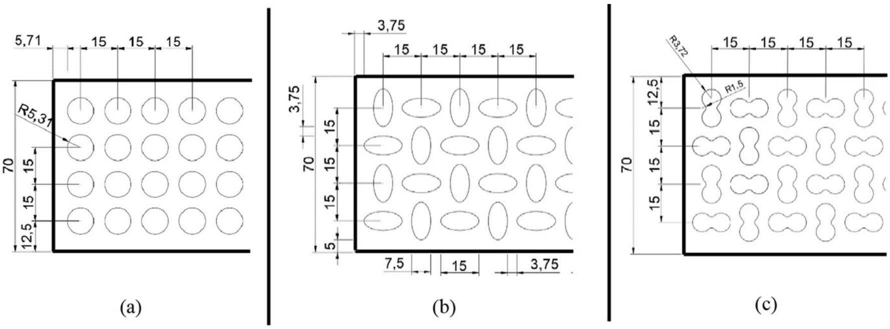

Fig. 1 Dimension details of (**a**) circular-perforated, (**b**) elliptic-perforated and (**c**) peanut-perforated mild steel sheets. All dimensions are in mm

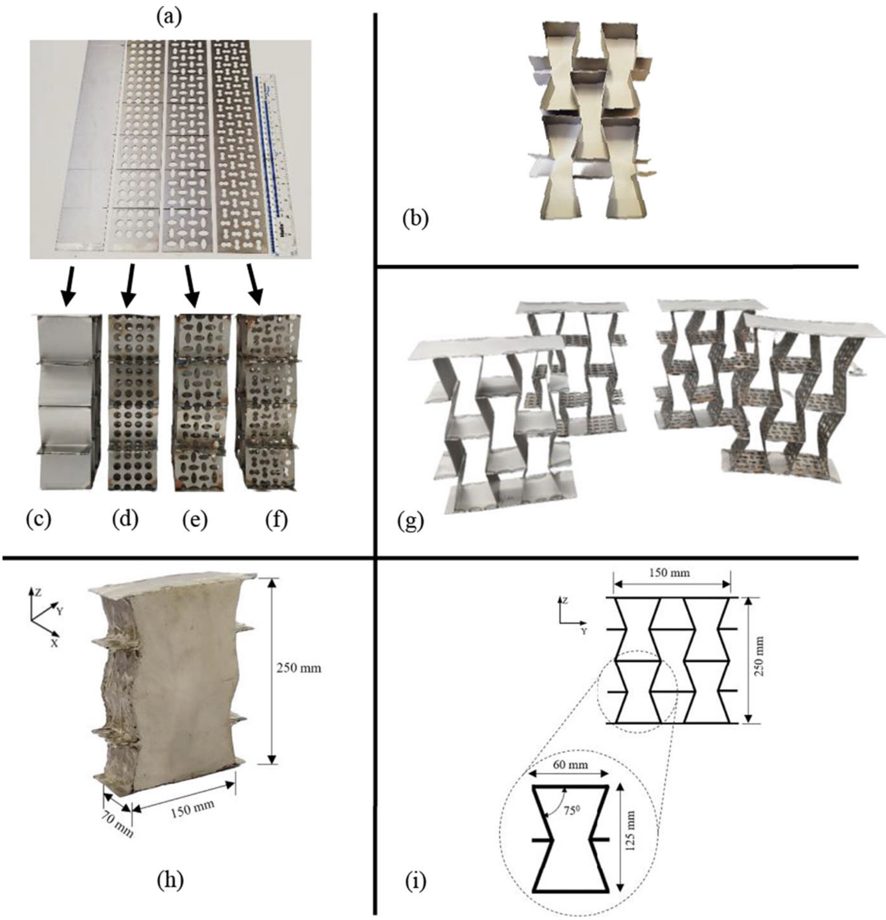

Fig. 2 (**a**) Non-perforated and perforated mild steel strips; (**b**) folded strips into re-entrant shapes; side views of welded (**c**) non-perforated, (**d**) circular-perforated, (**e**) elliptic-perforated, (**f**) peanut-perforated re-entrant honeycomb structures; (**g**) some welded re-entrant meshes; (**h**) mesh-mortar composites; (**i**) dimension details of re-entrant structure

the bottom of each auxetic structure in order to contain the mortar within the structure during casting (see Fig. 2g).

2.2 Mortar

The materials used for the mortar were Hanson general-purpose cement (32.5R) and natural sand that complies with the ASTM C33/C33M as sharp concreting sand. The sand with 4 mm maximum aggregate size together with the cement were all obtained

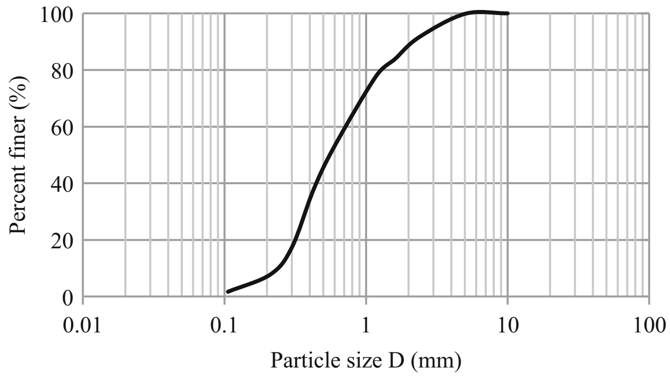

Fig. 3 Particle size distribution of sharp sand used for the cement mortar

from Jewson Exeter, UK. The mortar consisted of the binder and aggregate in 1:5 mix ratio while the water/cement ratio was 0.48 [18]. Sikamix mortar plasticiser was added to the water at a dosage of 2.5 ml plasticiser per kg of cement before mixing with the aggregates. The binder and aggregate were first dry-mixed in a rotating drum after which the measured water containing mortar plasticiser was added. The mixing continued for 5 min, following the requirements of ASTM C33/C33M until a consistent mix was achieved. Figure 3 presents the particle size distribution. The external side of the outer walls of the honeycomb were covered with transparent stick tape (Sellotape) to avoid the concrete seeping through. The re-entrant honeycomb structures were then placed on a flat wooden plate and held onto the plate using steel wires. The mortar was then poured into the plate and vibrated for about 2 min and left undisturbed for 24 h. At the end of the 24 h period, the sticky tapes were removed, and the honeycomb–concrete composites were transferred into a water tank and cured under ambient temperature for 28 days prior to testing.

2.3 Tensile Strength Test

The perforated and non-perforated strips were tested in tension to investigate their tensile capacities and auxetic behaviour. The tensile strength test was carried out in displacement control (at 5 mm/min) in an Instron 34TM-30 universal testing machine, according to ASTM A370 – 11. Figure 4 shows images of some of the tensile test samples before and after testing. The Poisson's ratios of the samples were calculated by obtaining six (6) lateral width measurements along each sample length before and after the tensile test, using a digital vernier caliper and dividing the change in the average final width by the change in the final longitudinal length of each sample.

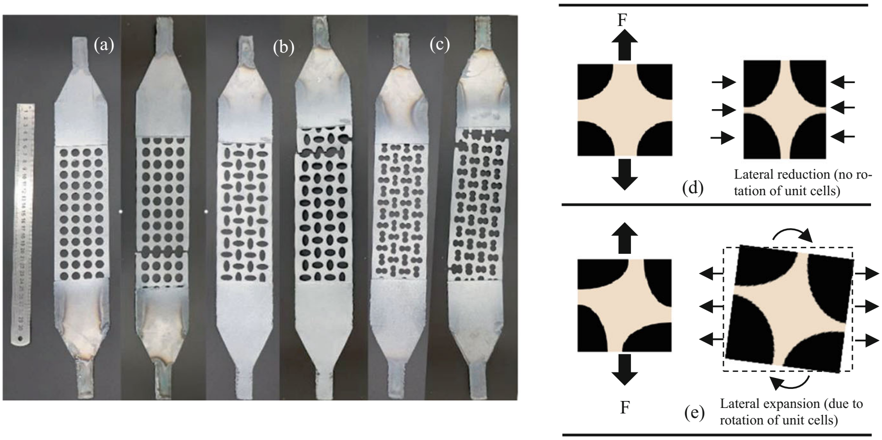

Fig. 4 (**a**) Circular-perforated, (**b**) elliptic-perforated and (**c**) peanut-perforated mild steel samples before and after tensile strength test; (**d**) illustration of positive Poisson's ratio for circular perforated samples; and (**e**) negative Poisson's ratio for elliptic perforated samples

2.4 Compressive Strength Test

The mortar-filled auxetic composites were tested in compression in compliance with ASTM C39 in displacement control at 5 mm/min. The test was stopped after a travel distance of 75 mm.

3 Results and Discussion

3.1 Tensile Strength Test of Perforated Mild Steel Strips

While the circular-perforated samples underwent reduction in the lateral direction, the elliptic- and peanut-perforated samples expanded in the lateral direction, hence indicating NPR (see Fig. 4). The overall behaviour of the samples was governed by the resistance mechanism of each constituting unit cell. For the circular-perforated samples, the axial tension force from the machine was resisted by the material in between the holes with direct axial straining and yielding until failure. Conversely, the orthogonal arrangement of holes in the elliptic- and peanut-perforated sheets, provided alternating material paths for load resistance, hence, causing the rotation of the unit cells (see Fig. 4d, e). The rotations of the cells caused an increase in the lateral dimension until the cells were aligned in the vertical axis of loading.

It was after this alignment, that the cells began to strain and yield in the axial direction of loading subsequently with some strain-hardening until failure. Consequently, the circular-perforated samples possessed relatively higher stiffness and

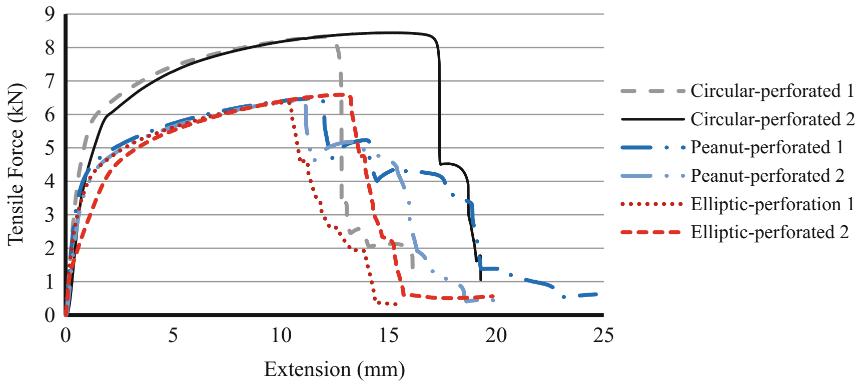

Fig. 5 Tensile strength curves of the perforated steel sheets

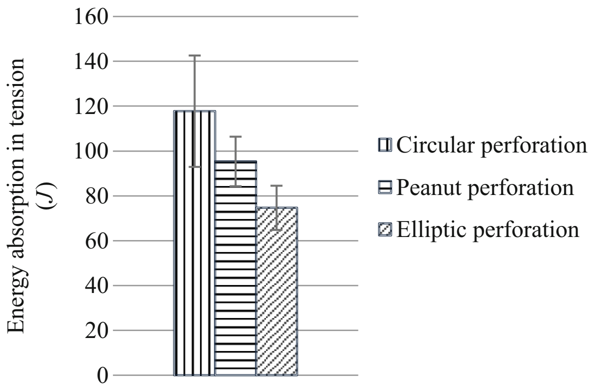

Fig. 6 Energy absorption from tensile strength curves of the perforated steel sheets

tensile strength as shown in Fig. 5. Average tensile capacities and Poisson's ratios of 8.39 kN, 6.47 kN, and 6.44 kN and −0.214, −0.246, and 0.279 were obtained for circular-, elliptic- and peanut-perforated samples, respectively. The variation between individual tensile test strip samples of the same category is due to possible inconsistencies in the perforations as well as in the testing procedure.

A simple uniaxial tensile strength test alone is not sufficient to account for energy dissipation through rotation of the unit cells of the auxetic strips; therefore, the circular-perforated strips seemed to possess more energy absorption (i.e. the area under the load–extension curve). Although the difference in average tensile capacities between the elliptic- and peanut-perforated samples is negligible, the average energy absorption of the latter is about 28% greater due to its relatively higher NPR (see Fig. 6). It is also important to note that only two samples each were tested for tensile strength behaviour for each category of perforated strip. This small sample size is a limitation and will be increased in future studies.

3.2 Compressive Strength Test

Generally, the stress–strain behaviour of re-entrant honeycomb structures is characterised by three major regimes: the linear elastic stage, the softening or plateau stage and the densification/destruction stage [19]. However, in this study, at the start of loading, the compressive load on the auxetic steel-mortar composite, increased linearly with displacement. The slope of the load–displacement curve then reduces at the onset of cracking within the mortar (see Fig. 7). Nevertheless, the capacity of the samples increased until excessive cracking within the mortar resulted in the rapid reduction of the load–displacement curve. This rapid reduction in capacity is followed by a plateau regime, which further evolves into the densification of the composite with subsequent crushing/destruction. The crushing stage succeeded the densification stage with concrete spalling from the cells of the auxetic meshes as depicted in Fig. 8.

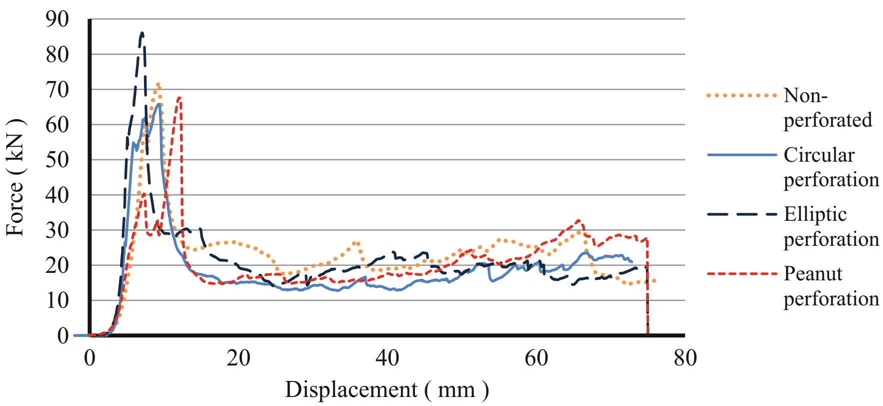

Fig. 7 Compressive behaviour curves of samples with the maximum compressive strengths for non-perforated and perforated re-entrant honeycombs

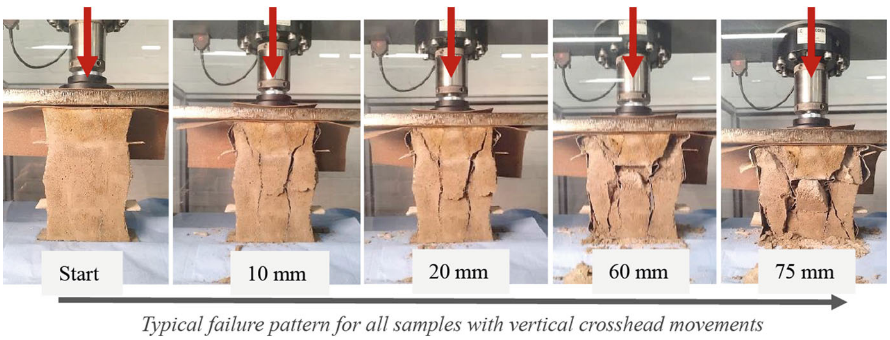

Fig. 8 Compressive strength testing of non-perforated and perforated re-entrant honeycomb–mortar composites

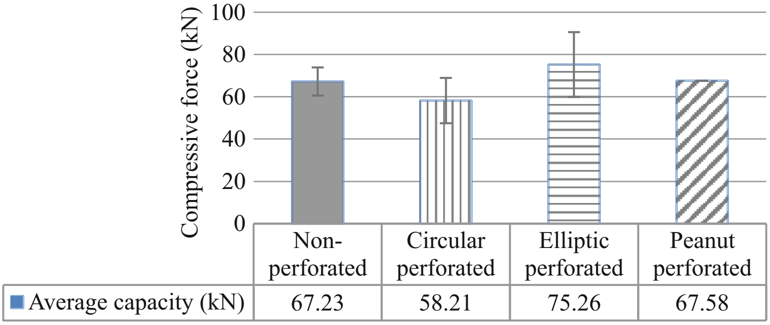

Fig. 9 Average compressive strengths of non-perforated and perforated re-entrant honeycombs

Figure 7 is the compressive behaviour curves of selected samples having maximum compressive capacities for non-perforated and perforated re-entrant honeycombs–mortar composites. Figure 9 presents the average compressive capacities (with standard deviations) of all the categories. Due to the enhanced bonding and the auxetic action provided by the perforations, the average compressive capacity of the elliptic-perforated samples increased by about 12% and 19% compared with the unperforated and circular-perforated samples, respectively. The compressive capacity of the peanut-perforated sample was greater than the circular-perforated samples by about 17%. However, there was negligible improvement in the compressive capacity of the peanut-perforated samples compared with the unperforated samples. This could be attributed to the trapping of larger grains of aggregates in between the 'neck' of the peanut perforation, thereby creating weak zones within the composite. The respective energy absorption for the samples was calculated using Eq. (1).

$$\int_0^l F dl \tag{1}$$

where F is the applied load (in kN) and l is the corresponding displacement (in mm).

The amount of steel used for each perforated steel–mortar composite category is exactly half the mass of the steel used for the non-perforated samples. According to Eq. (2), this corresponds to a 50% mass consumption ratio (TMCR) for the perforated samples [20]. Recent studies show that cellular auxetic structures can be obtained with up to 34% of material in comparison with their homogeneous counterparts [20]. Although the process of perforation could result in extra costs, advancements in manufacturing technologies could offset these costs allowing for innovative engineering load bearing applications.

$$\mathrm{TMCR} = \frac{\text{mass of auxetic component}}{\text{mass of homogeneous component}} \times 100\% \tag{2}$$

The different samples can also be compared using Eq. (3) which specifies a dimensionless design optimisation factor (Df) [20]:

$$Df = \frac{k}{\text{displacement} \times \text{TMCR}} \times 100\%, \tag{3}$$

where k is empirically chosen as 1 and having the same unit as the displacement (or strain, deformation, rotation, etc.) [21]. In this study, the highest Df resulted from the auxetic reinforcements. These are the samples with the highest compressive capacity and use the least amount of steel reinforcement (i.e. the elliptic- and peanut-perforated samples). The Df of the perforated samples are more than that of the non-perforated samples with values of 9.3, 25.5, 19.4 and 16.5 for non-perforated, circular-perforated, elliptic-perforated and peanut-perforated samples respectively. Parameters such as TMCR and Df can be used as selection tools for the dimensions of perforation and for the design of other components. For components in flexure, the displacement in Eq. (3) can be replaced with deflection or strain. Although the normalised average energy absorption from the compressive strength curves was highest for the non-perforated samples (Fig. 10), it should be noted that the perforated samples have exactly 50% less steel reinforcement.

The perforated steel re-entrant honeycomb-reinforced mortar composite developed in this study can be used for applications such as lightweight beams, columns, sandwich panels and shear walls. The perforations improve bonding between the reinforcement and matrix through continuity of the matrix as well as through the NPR of the steel sheets. Such composite also does not require additional formwork for making them since the cellular arrangement can keep the wet concrete in place. Further studies are however required to investigate the effects of perforation parameters such as aspect ratio and angular orientation of the holes in order to tailor them for specific load-bearing components. The next stage of this research involves investigations on the mechanical behaviour on a larger sample size in order to enhance the rigor and impact of the results.

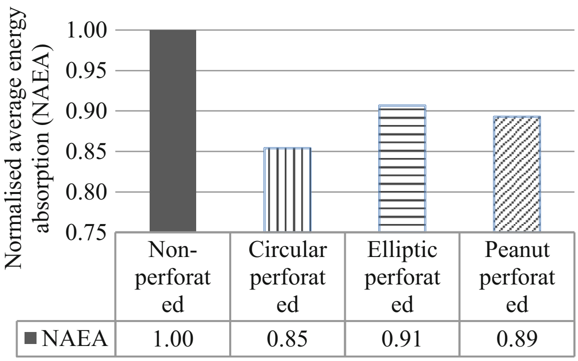

Fig. 10 Normalised average energy absorption for all perforated samples under compression

4 Conclusions

This paper focused on the behaviour of perforated re-entrant auxetic steel honeycomb–mortar composite. The need to improve the bond strength between steel and concrete through auxeticity led to the orthogonal perforation of the steel strips. The tensile strength behaviour of the steel strips was assessed as well as the compressive strengths of the respective composites with circular, elliptic and peanut orthogonal perforations in the re-entrant steel honeycomb. Consequently, the following key findings are highlighted:

- The tensile capacities of circular-perforated sheets are over 29% greater than those of the orthogonal elliptic- and peanut-perforated sheets.
- The difference in average tensile capacities between the elliptic- and peanut-perforated samples is negligible; however, the average energy absorption of the latter is about 28% greater.
- Due to the enhanced bonding and the auxetic action provided by the perforations, the average compressive capacity of the elliptic-perforated samples is about 12% and 19% greater than that of the unperforated and circular-perforated samples.
- Parameters such as the 'design optimisation factor' and 'total mass consumption ratio' can be used to select the optimum dimensions for perforations.
- The perforated steel sheets use only 50% of the material constituting the non-perforated steel sheets, implying that introducing auxeticity through perforations can reduce overall material usage. This can offer benefits in specialised steel-reinforced cementitious load bearing applications such as concrete shear walls.

Acknowledgement and Funding This work was supported by the United Kingdom's Engineering and Physical Sciences Research Council (EPSRC, UK), [EP/W019027/1].

Conflicts of Interest The authors have no conflicts of interest to declare that are relevant to the content of this article.

Data Access Statement Data will be made available on request.

References

1. Xu, Y., Šavija, B.: Architected cementitious cellular materials: peculiarities and opportunities. Heron. **66**(2–3), 239–271 (2021)
2. Rosewitz, J.A., Choshali, H.A., Rahbar, N.: Bioinspired design of architected cement-polymer composites. Cem. Concr. Compos. **96**, 252–265 (2019)
3. Momoh, E.O., Osofero, A.I., Oleksandr, M.: Behaviour of clamp-enhanced palm tendons reinforced concrete. Constr. Build. Mater. **341**, 127824 (2022)

4. Oggeri, C., Ronco, C., Vinai, R.: Validation of numerical D.E.M. modelling of geogrid reinforced embankments for rockfall protection. Geoing. Ambient. Mineraria. **58**(2(3)), 36–45 (2021)
5. Mukhopadhyay, S., Khatana, S.: A review on the use of fibers in reinforced cementitious concrete. J. Ind. Text. **45**(2), 239–264 (2014)
6. Momoh, E.O., Osofero, A.I., Menshykov, O.: Physicomechanical properties of treated oil palm-broom fibers for cementitious composites. J. Mater. Civ. Eng. **32**, 04020300 (2020)
7. Momoh, E.O., Osofero, A.I., Menshykov, O.: Bond behaviour of oil palm broom fibres in concrete for eco-friendly construction. Proc. Inst. Civ. Eng.-Constr. Mater. **174**(1), 47–64 (2021)
8. Luo, C., Han, C.Z., Zhang, X.Y., Zhang, X.G., Ren, X., Xie, Y.M.: Design, manufacturing and applications of auxetic tubular structures: a review. Thin-Walled Struct. **163**, 107682 (2021)
9. Xu, Y., Schlangen, E., Lukovic, M., Savija, B.: Tunable mechanical behavior of auxetic cementitious cellular composites (CCCs): experiments and simulations. Constr. Build. Mater. **266**(B), 121388 (2021)
10. Subramani, P., Rana, S., Oliveira, D.V., Fangueiro, R., Xavier, J.: Development of novel auxetic structures based on braided composites. Mater. Des. **61**, 286–295 (2014)
11. Zahra, T., Dhanasekar, M.: Characterisation of cementitious polymer mortar – auxetic foam composites. Constr. Build. Mater. **147**, 143–159 (2017)
12. Peliński, K., Smardzewski, J.: Static response of synclastic sandwich panel with auxetic wood-based honeycomb cores subject to compression. Thin-Walled Struct. **179**, 109559 (2022)
13. Momoh, E.O., Jayasinghe, A., Hajsadeghi, M., Vinai, R., Evans, K.E., Kripakaran, P., Orr, J.: A state-of-the-art review on the application of auxetic materials in cementitious composites. Thin-Walled Struct. **196**, 111447 (2024)
14. Ren, X., Shen, J., Ghaedizadeh, A., Tian, H., Xie, Y.M.: A simple auxetic tubular structure with tuneable mechanical properties. Smart Mater. Struct. **25**, 065012 (2016)
15. Zhong, R., Ren, X., Zhang, X.Y., Luo, C., Zhang, Y., Xie, Y.M.: Mechanical properties of concrete composites with auxetic single and layered honeycomb structures. Constr. Build. Mater. **322**, 126453 (2022)
16. Zhou, H., Jia, K., Wang, X., Xiong, M.-X., Wang, Y.: Experimental and numerical investigation of low velocity impact response of foam concrete filled auxetic honeycombs. Thin-Walled Struct. **154**, 106898 (2020)
17. Luo, C., Ren, X., Han, D., Zhang, X.G., Zhang, R., Zhang, X.Y., Xie, Y.M.: A novel concrete-filled auxetic tube composite structure: design and compressive characteristic study. Eng. Struct. **268**, 114759 (2022)
18. Bouaich, F.Z., Maherzi, W., Benzerzour, M., Taleb, M., Abriak, N.-E., Rais, Z., Senouci, A.: Mortar mixing using treated wastewater feasibility. Constr. Build. Mater. **352**, 128983 (2022)
19. Alomarah, A., Masood, S.H., Sbarski, I., Faisal, B., Gao, Z., Ruan, D.: Compressive properties of 3D printed auxetic structures: experimental and numerical studies. Virtual Phys. Prototyp. **15**, 1–21 (2020)
20. Menon, H.E., Dutta, S., Krishnan, A., Hariprasad, M.P., Shankar, B.: Proposed auxetic cluster designs for lightweight structural beams with improved load bearing capacity. Eng. Struct. **260**, 114241 (2022)
21. Baumers, M., Dickens, P., Tuck, C., Hague, R.: The cost of additive manufacturing: machine productivity, economies of scale and technology-push. Technol. Forecast. Soc. Chang. **102**, 193–201 (2016)

Open Access This chapter is licensed under the terms of the Creative Commons Attribution 4.0 International License (http://creativecommons.org/licenses/by/4.0/), which permits use, sharing, adaptation, distribution and reproduction in any medium or format, as long as you give appropriate credit to the original author(s) and the source, provide a link to the Creative Commons license and indicate if changes were made.

The images or other third party material in this chapter are included in the chapter's Creative Commons license, unless indicated otherwise in a credit line to the material. If material is not included in the chapter's Creative Commons license and your intended use is not permitted by statutory regulation or exceeds the permitted use, you will need to obtain permission directly from the copyright holder.